Cytometry Part A 57A:120–130 (2004)

Rapid Communication

Quantitation of MHC Tetramer-Positive Cells From Whole Blood: Evaluation of a Single-Platform, Six-Parameter Flow Cytometric Method

Matthias Wölfl,[1]* Stefan Schalk,[1] Martin Hellmich,[2] Katharina M. Huster,[3] Dirk H. Busch,[3] and Frank Berthold[1]

[1]Children's Hospital, Department of Pediatric Hematology and Oncology, University of Cologne, Cologne, Germany
[2]Institute of Medical Statistics, Informatics and Epidemiology, University of Cologne, Cologne, Germany
[3]Institute for Medical Microbiology, Immunology and Hygiene, Technical University of Munich, Munich, Germany

Received 30 April 2003; Revision Received 5 June 2003; Accepted 16 October 2003

Background: Quantitation of antigen-specific T cells provides an insight into the development and dynamics of T-cell responses in tumor immunology and infectious diseases. Soluble major histocompatibility class I tetramers are widely used to monitor immune responses; however, variations due to handling and analysis are likely to confound comparisons between different experiments and laboratories.

Methods: Whole blood from healthy donors was stained with HLA-A*0201/tetramers specific for an epitope of phosphoprotein 65, the immunodominant antigen in cytomegalovirus infection. With the help of Trucount tubes, a single-platform, four-color flow cytometric assay was established to obtain absolute counts of tetramer-positive cells. Various staining and gating strategies were evaluated.

Results: The no-wash method was a quick and straightforward procedure for the quantitation of tetramer-positive events from whole blood. The level for background staining was low. This information about the intra-assay–related variation and the physiologic variation will allow validation and interpretation of data in future studies.

Conclusions: The method is highly reliable and can be standardized for multiple experiments. It is therefore suitable for the direct ex vivo analysis of antigen-specific T cells in a variety of clinical settings such as infectious, autoimmune, or neoplastic diseases and can be implemented as a tool for multicenter studies. © 2004 Wiley-Liss, Inc.

Key terms: MHC tetramers; antigen-specific T cells; cytomegalovirus; flow cytometry; single-platform

Soluble major histocompatibility class (MHC) I tetramers are widely used in tumor immunology and infectious diseases to monitor antigen-specific immune responses (1,2). Tetramers are specific for the relevant T-cell receptor and, hence, allow detection of low frequencies of peptide-specific $CD8^+$ T lymphocytes. Quantitation of rare cells is dependent on the accuracy and precision of the assay (3). Accuracy and precision strongly depend on the amount of background staining and on handling artifacts, i.e., those due to freezing and thawing. Values for the quantitation of rare cells are commonly given as the percentage of $CD8^+$ cells. Normalization for $CD8^+$ cells reduces variations due to the T-cell counts but can confound comparisons between different donors, experiments, or laboratories, if the gating strategy is not clearly defined.

The enumeration of rare cells has been standardized in clinical settings for $CD34^+$ cells, which are isolated for patients undergoing autologous stem cell transplantation, and for $CD4^+$ T cells for the immune monitoring of patients with the human immunodeficiency virus (HIV). Different groups have established protocols and guidelines using dual- or single-platform assays to obtain absolute cell counts (4–10). Flow cytometric single-platform methods are based on the use of a known number of fluorescent beads in the sample, containing a defined

Contract grant sponsor: Kinderkrebs-Neuroblastomforschung e.V.; Contract grant sponsor: Köln Fortune; Contract grant sponsor: Clinical Cooperation Vaccinology.

*Correspondence to: Matthias Wölfl, M.D., University of Cologne, Department of Pediatric Hematology and Oncology, Joseph-Stelzmann-Str. 9, 50924 Köln, Germany.
E-mail: matthias.woelfl@medizin.uni-koeln.de

volume. The number of the beads acquired allows for the calculation of the acquired volume per probe.

In this study, we establish and validate a single-platform flow cytometric assay to obtain absolute numbers of MHC tetramer-positive T cells from whole blood. Phosphoprotein 65 (pp65), the immunodominant protein of the cytomegalovirus (CMV) (11), is used as a model antigen in our system. Infection with CMV is persistent in healthy individuals and results in a robust immune response. In immunosuppressed patients, e.g., after organ transplantation, CMV is highly pathogenic and may lead to vasculitis or transplant failure among other disease manifestations (12,13). The monitoring of CMV-specific T cells therefore might help to predict whether the immune system can cope with the viral load (14–27). The method presented here allows for a standardized and direct quantitation of tetramer-positive, CMV-specific T cells in whole blood as absolute numbers and as a percentage of $CD8^+$ cells.

METHODS AND MATERIALS

Donors

Blood was obtained from healthy donors with a known HLA-A*0201 expression. Written informed consent was obtained from each subject. Blood was collected and mixed immediately with sodium heparin (10 U/ml blood). Seropositivity for CMV immunoglobulin G was tested by the Institute of Virology, University of Cologne, using standard enzyme-linked immunosorbent assay techniques.

Antibodies

The following antibodies were used: anti-CD3 fluorescein isothiocyanate (FITC; clone UCHT1), anti-CD8 peridinin chlorophyll protein (PerCP; clone SK1), anti–CD19-APC (clone HIB19), anti–CD45-APC (clone HI30), anti–CD56-APC (clone B159; all from BD Pharmingen, Heidelberg, Germany), anti–CD14-APC (clone TüK4), and anti–CD16-APC (clone 3G8; Caltag, Hamburg, Germany).

Tetramers

MHC multimer reagents were generated as previously described (21,28–30). Briefly, recombinant β2 microglobulin and HLA fusion proteins containing a specific biotinylation tag (31) at the C-terminus of the α3 domain were separately expressed as inclusion bodies in *Escherichia coli* (28). After purification of recombinant proteins, MHC molecules were folded in vitro in the presence of high concentrations of the relevant peptide. After enzymatic biotinylation (BirA), correctly folded and biotinylated MHC molecules were purified by chromatography over a size exclusion column (Superdex 200HR, Pharmacia, Uppsala, Sweden). Biotinylation efficiency was determined by avidin shift assay and reached greater than 95% for all reagents used in this study. Tetramerization was achieved by overnight incubation of biotinylated MHC molecules with streptavidin phycoerythrin (PE; Molecular Probes, Leiden, Netherlands) at a molar ratio of 5:1. Unbound MHC molecules were removed by washing MHC tetramers over a 100-kDa molecular weight cutoff spin tube membrane. MHC tetramers were concentrated to 2 mg/mL in phosphate buffered saline (pH 8) and stored at 4°C in the presence of protease inhibitors (pepstatin, leupeptin), ethylene diamine tetraacetic acid (1 mmol/L), and sodium azide (0.02%). The following synthetic peptides (Affina, Berlin, Germany) were used: pp65(495–503) (NLVPMVATV) and pol 476–484(ILKEPVHGV). Throughout all the experiments described in this study, the same batch of tetramers was used. Specificity of the tetramers was controlled by staining of peptide-specific T-cell clones (data not shown).

Staining

An aliquot of whole blood with heparin was pipetted into 1.5-ml reaction tubes. For all assays (except for the titration assay), a concentration of 0.2 μg of tetramer per 100 μl whole blood was used. The tetramer was added, and the probe was vortexed and incubated for 20 min at room temperature. An antibody mixture containing CD3-FITC, CD8-PerCP, CD56-APC, CD19-APC (10 μl of each antibody/100 μl blood), CD16-APC, and CD14-APC (2.5 μl/100 μl blood) was added and incubated for another 15min at room temperature. In some experiments CD45-APC was used instead of the APC-labeled exclusion cocktail. Initial experiments included samples incubated with FITC-, PerCP-, and APC-labeled isotype control immunoglobulin G_1 (BD Pharmingen).

Nine hundred microliters of FACS lysing solution (BD Pharmingen) was pipetted into Trucount tubes (BD Pharmingen). By using a reverse pipetting technique, 145 μl of the antibody–blood mixture (100 μl of blood and 45 μl of the antibody mixture) was added to the Trucount tubes. Samples were vortexed, incubated for 15 min at room temperature, and then put on ice for immediate analysis. Each probe was stained in one tube and then measured as duplicates in two separate Trucount tubes.

Data Acquisition, Instrument Settings, and Sequential Gating

Data were acquired using a FACScalibur with an additional 635-nm red diode laser for the fourth color. Analysis was carried out with CellQuest Pro (BD Pharmingen) software. Acquisition was performed by gating on beads. Because light scatter appearance is not recommended for gating on beads, two regions (R6 and R7) were routinely used, taking into account all four colors of the beads (Fig. 1, plots 1 and 2). Events that were positive for all four colors were regarded as beads (G4 = R6 and R7). The number of the beads per tube varies from batch to batch and is indicated individually for each batch by the manufacturer. Acquisition was stopped when one-third of the beads was counted (in general, approximately 18,000 beads). For acquisition, a CD3 anchor was used by setting the threshold of FL1 on 200.

Light scatter parameters were amplified to best visualize lymphocytes. The color compensation between different fluorochromes was set with single fluorochrome-stained cells and the appropriate isotype-labeled controls by using the same staining procedure described earlier.

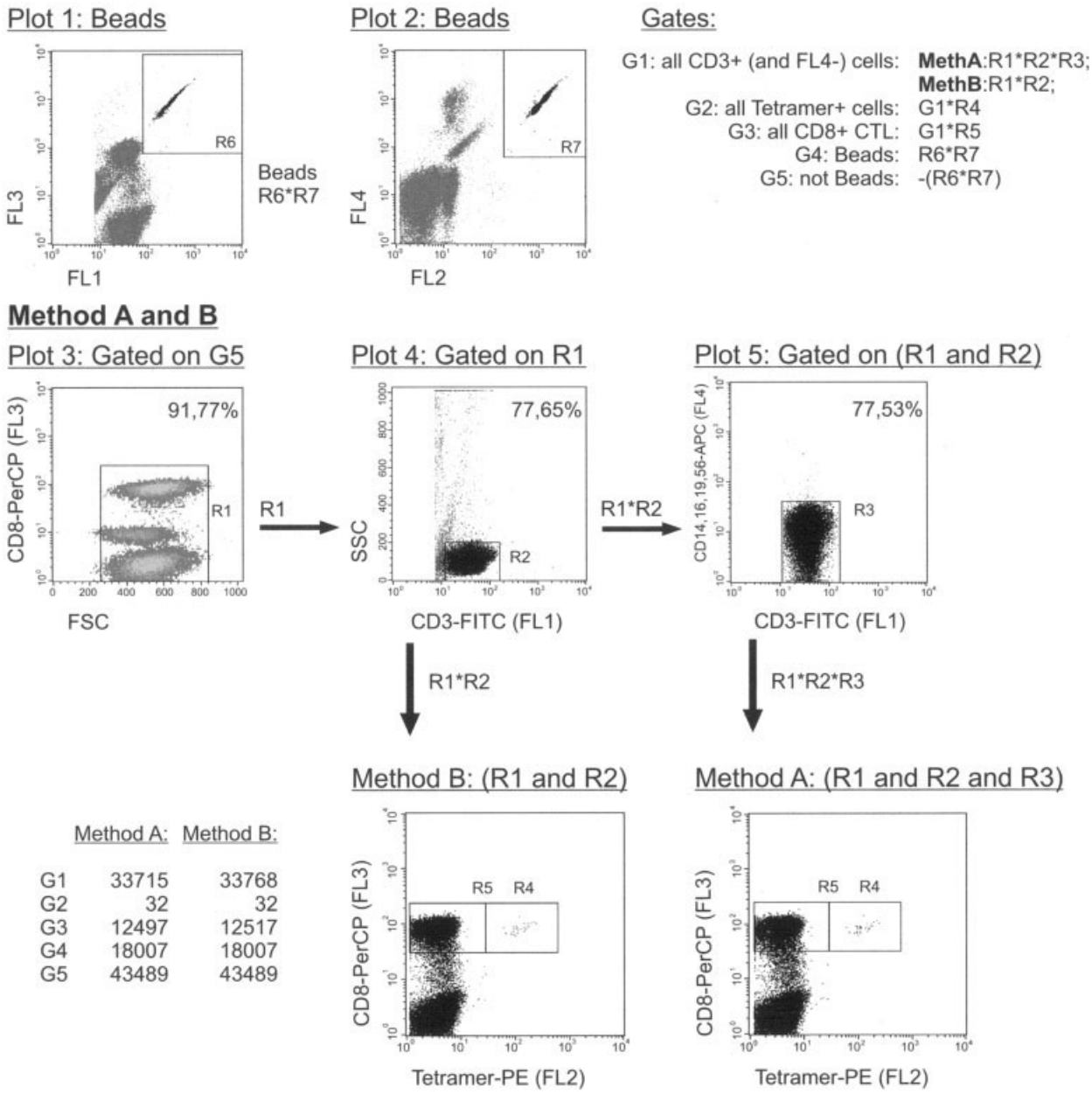

FIG. 1. Data acquisition and sequential gating using Trucount tubes and staining with anti–CD3-FITC, tetramer-PE, anti–CD8-PerCP, anti–CD14-APC, anti–CD16-APC, anti–CD19-APC, and anti–CD56-APC on whole blood. List mode data were acquired on a FACScalibur (BD Biosciences) and analyzed with CellQuest Pro software. Standard method (method A): Plots 1 and 2: Acquisition was performed by gating on beads. Beads are identified by combining R6 and R7 (= G4). Acquisition was stopped when one-third of all beads was counted. Plot 3: All events (beads excluded) are displayed in a density plot of FSC versus FL3(CD8). R1 includes more than 95% of the $CD8^+$ population. Plot 4: All events from R1 are displayed in an FL-1(CD3) versus SSC dot plot. R2 includes $CD3^+$ cells with a low SSC. Plot 5: Cells from R1 and R2 are displayed in an FL1(CD3) versus FL4 dot plot to exclude all $FL4^+$ cells (CD14,CD16,CD19,CD56) (R3). Method A: All cells from R1 and R2 and R3 (= G1) are displayed in an FL2(tetramer) versus FL3(CD8) dot plot. R4 defines tetramer-positive events. Absolute numbers are defined by G2 = G1 and R4. Absolute numbers for $CD8^+$ cells are defined by G3 = G1 and R5. Alternative gating strategy (method B, no exclusion gate): All cells from R1 and R2 are displayed directly in an FL2(tetramer)/FL3(CD8) dot plot. Percentages indicate the numbers of the cells within the region of interest versus all cells (beads excluded). Instrument settings remained unchanged for all experiments.

Analysis was performed by excluding all beads (Fig. 1, G5). All remaining cells were displayed in an forward scatter (FSC)/FL3(CD8) density plot, and a region was drawn to determine the upper and lower FSC bounds of the $CD8^+$ population (Fig. 1, R1, plot 3). These cells were then displayed in an FL1 (CD3)/side scatter (SSC) dot plot, and a region was drawn around the $CD3^+$ population with a low side scatter (Fig. 1, R2, plot 4). Gating on cells in R1 and R2 in an FL1(CD3)/FL4 dot plot revealed all contaminating cells that were positive for any of the markers such as CD14, CD16, CD19, or CD56. A region (R3) including all $FL4^-$ cells was drawn (plot 5). Combining these three

regions in one gate (G1 = R1 and R2 and R3) displayed all $CD3^+CD14^-CD16^-CD19^-CD56^-$ lymphocytes with a typical light scatter appearance. These cells were then displayed in an FL2(tetramer)/FL3(CD8) dot plot, and a region around tetramer-positive, CD8 highly positive cells was drawn (R4, plot 6). Gate 2 then combined G1 and R4 to produce the absolute number of tetramer-positive, $CD8^+$ T cells. An additional region (R5) could be used to quantitate the number of $CD8^+$ T cells (G1 and R5). This gating method was used as the standard method, referred to as *method A*.

An alternative approach, referred to as *method B*, was evaluated in some experiments. For this approach the exclusion gate was omitted, i.e., gating was performed on R1 and R2 and cells were directly displayed in an FL2(tetramer)/FL3(CD8) dot plot (Fig. 1, method B). In a third approach, all cells (beads excluded) were displayed directly in a FL1(CD3)/FL4(CD14/CD16/CD19/CD56) dot plot, and $CD3^+FL4^-$ cells were displayed in the FL2(tetramer)/FL3(CD8) dot plot (method C).

Calculation of the absolute amount of tetramer-positive cells per microliter of whole blood was done with the following equation:

$$(\text{n tetramer-positive cells acquired [gate 2]} \times \text{n beads/Trucount tube})/(\text{n beads acquired [gate 4]} \times \text{volume sample[} = 100\mu\text{l]})$$

Analysis of Mean Fluorescence Intensities

To compare the mean fluorescence intensity (MFI) of positive events with the negative population, a widely accepted way is to use the so-called 2% threshold method (32). Briefly, a 2% threshold marker is set in a control histogram containing 2% of the cells with the highest fluorescent intensity. This marker is then applied for positive samples, and the values of the positive and the negative sample can be subtracted or correlated to each other. Because we expected low amounts of positive cells, we used a 1% threshold, which is sufficient to include all positive events. Further, rather than pre-setting the threshold in the negative control sample (e.g., stained with HIV tetramer), we analyzed samples individually, adapting the markers of the "threshold gate," so that the top 1% of each sample was included. The x-fold increase was then calculated as (MFI of top 1% − MFI of all cells)/MFI of all cells. This calculation allows for the comparison of the MFI of the 1% of cells with the highest fluorescence intensity with the MFI of all cells of the sample and can be applied for each sample individually.

Statistics

Assay accuracy was assessed as part of the "limits of agreement" approach suggested by Bland and Altman (33) and by least-squares linear regression analysis where the intercept parameter can be interpreted as constant bias and the difference "1 minus slope parameter" as proportional bias (3). Assay precision was assessed by calculation of variance components (between tubes, within tubes) or, when the assumption of normal distributed data was implausible, by determination of maximal individual 99% quantiles (background) or mean relative ranges (variation over time), i.e., (99% quantile − median)/median averaged over patients. Assay linearity was assessed by least-squares linear regression analysis (slope, y intercept, R^2, residual standard deviation).

Statistical analyses were performed with R 1.6.2 and Microsoft Excel 2000.

RESULTS

Titration of Tetramers Is Required for Optimal Resolution of Positive and Negative Events

In a first series of experiments, $CMVpp(65)_{(495–503)}$ tetramer was titrated with the blood of $HLA\text{-}A^*0201^+/CMV^+$ donors at a concentration of 0.1–0.8 μg/100 μl whole blood.

A high resolution between positive and negative events could be achieved with as little as 0.2 μg/probe. In two of three experiments, the MFI of negative cells increased with the increasing concentration of the tetramer. To avoid bias due to gating on positive and negative events, we applied the modified threshold method as described in Materials and Methods to calculate the increase of fluorescence of the positive cells over the background. This calculation allows for a standardized analysis and comparison of the MFI of the positive and negative events, even if the fluorescence of the negative events varies from sample to sample. Comparison of the raw data (Fig. 2) and calculation of the x-fold increase of the top 1% of the cells per sample (upper right corner of each plot) showed 0.2 μg of tetramer/100 μl whole blood to be sufficient, resulting in optimal discrimination. This concentration was then used for all other assays.

Background, Detection Limit, Linearity, and Time Dependency

As described in Materials and Methods, the acquisition was stopped when one-third of the beads was counted. This equals 33.3 μl of the 100 μl whole blood. Given that there was no background staining at all, mathematically, one event per 33.3 μl, or three events per 100 μl, could be detected. The theoretical detection limit therefore is 0.01% of $CD8^+$ T cells, given that there are approximately 30,000 $CD8^+$ cells/100 μl in healthy donors. The detection limit can be improved by acquiring more of the sample (e.g., half of the beads), and doing so is reasonable, if extremely low frequencies are expected. However, by increasing the amount of events acquired, acquisition time is significantly increased.

The real detection limit depends on the background staining. Analysis of the probes stained with the $HIV(pol)_{(476–484)}$ tetramer in general revealed a low background (Table 1). To define a threshold above which the probes are considered to be positive, we performed repetitive stainings with the $HIV(pol)_{(476–484)}$ tetramer (two to six times) for each donor. Based on these data, we calculated the 99% quantile for each of the 14 donors

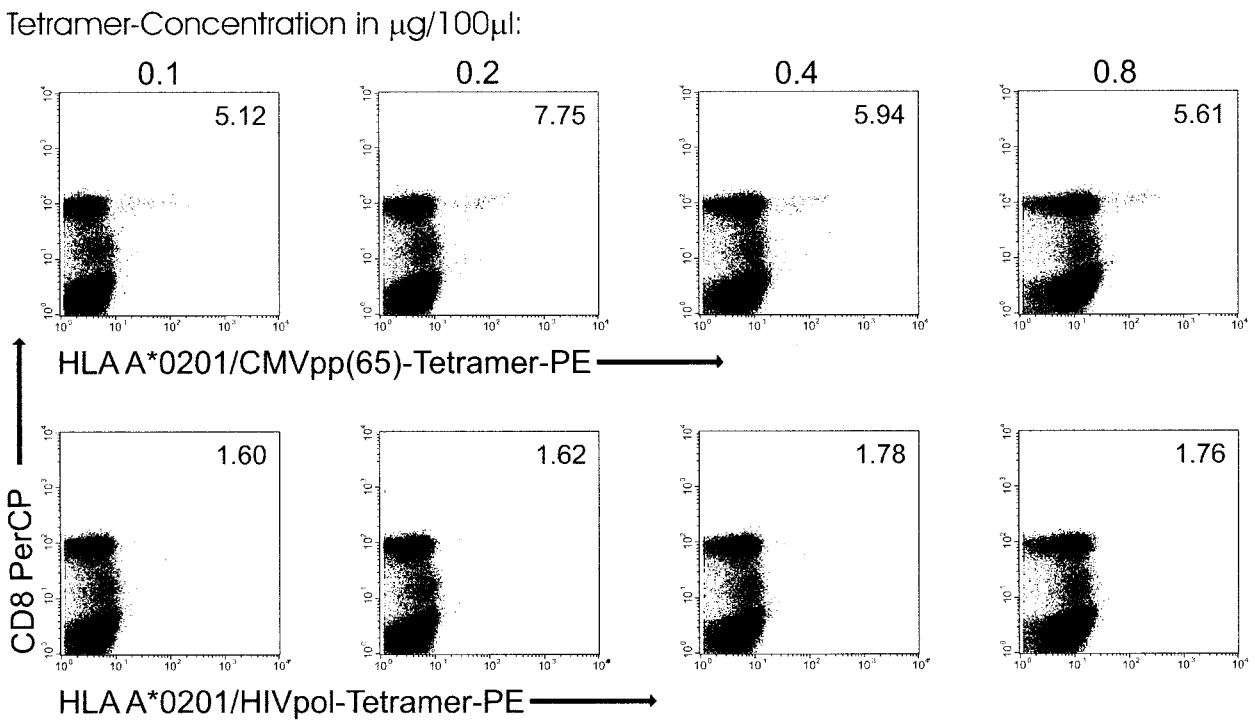

FIG. 2. Titration of the CMVpp(65)$_{(495-503)}$ tetramer (top row). Whole blood, 0.1–0.8 µg/100 µl, from HLA-A*0201$^+$/CMV$^+$ donors was stained. The x-fold increase of tetramer-positive over tetramer-negative CD8$^+$ cells was calculated as described in the text and is given in the upper right corner. Staining with HIV(pol)$_{(476-484)}$ tetramer is shown as a negative control (lower row). Plots represent one of three experiments.

individually and chose the donor with the highest value to determine the upper limit for the assay. The value of the highest 99% quantile was 13.95 cells/100 µl whole blood, or 38.69 cells/10^5 CD8$^+$ T cells (<0.04%). Staining of CMV$^-$ donors with CMVpp(65)$_{(495-503)}$ tetramer revealed similar intervals for the background (99% quantile, maximum: 8.93 cells/100 µl, or 17.51 cells/10^5 CD8$^+$ T cells; Table 1).

Table 1
*Determination of Background Staining for Individual Donors**

Patient no.	99% quantile HIV (pol)$^{(476-484)}$ tetramer		99% quantile CMVpp(65)$_{(495-503)}$ tetramer	
	Cells/100 µl whole blood	Cells/10^5 CD8$^+$ T cells	Cells/100 µl whole blood	Cells/10^5 CD8$^+$ T cells
1	5.98	20.76	—	—
2	**13.95**	26.76	—	—
3	11.22	34.28	—	—
4	9.97	**38.69**	—	—
5	8.27	14.35	—	—
6	2.99	7.74	—	—
7	2.89	5.34	8.58	14.22
8	8.90	17.36	0	0
9	2.96	6.83	2.96	6.96
10	8.90	12.71	8.90	12.98
11	2.90	5.57	8.59	13.28
12	0	0	0	0
13	2.96	5.75	**8.93**	**17.51**
14	0	0	8.90	12.18

*Blood from each donor was stained repeatedly (two to six times) with the respective tetramer. The 99% quantile was calculated for each donor. The highest background values (bold numbers) define the upper limit for negative samples. Patients 1 to 6 were CMV$^+$; therefore, the values for the staining with the CMV tetramer are not shown.

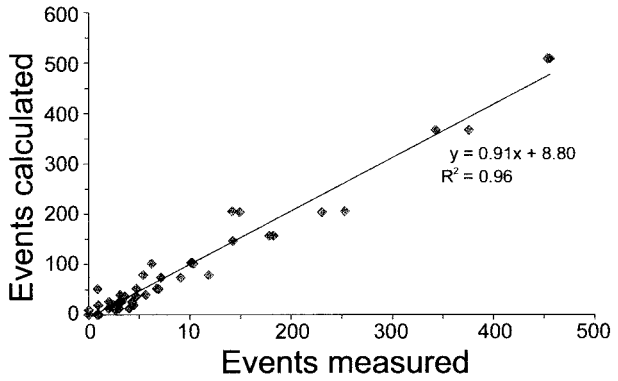

FIG. 3. Linear regression of statistically expected, measured quantity of cells showing high goodness-of-fit ($y = 0.91x + 8.8$; $R^2 = 0.964$; residual standard deviation: 29.62) limits of agreement were determined as described in Figure 5: mean ratio of (measured − expected)/expected: 0.17; standard deviation, 0.71). Cells stained with CMVpp(65)$_{(495-503)}$ tetramer were titrated to samples stained with HIV(pol)$_{(476-484)}$ tetramer. Expected values were calculated from samples stained with CMV tetramer and acquired as duplicates (= positive control, 100%). Data from four different experiments are included.

To assess linearity between expected and observed events, we performed mixing assays by titrating a positive probe stained with CMVpp(65)$_{(495-503)}$ tetramer into a negative probe stained with HIV(pol)$_{(476-484)}$ tetramer. A linear regression of statistically expected, measured quantity of cells showed high goodness of fit (Fig. 3); thus, the assay is assumed linear over the relevant measurement range.

Time course experiments showed a loss of positive events (in some experiments, up to 25%) within the same probe (on ice) after periods longer than 3 h (Fig. 4). This could not be stabilized by the addition of paraformaldehyde (0.33% final concentration; data not shown). Hence, we limited the acquisition time to 2 h, which allowed the analysis of a maximum of 12 samples per assay.

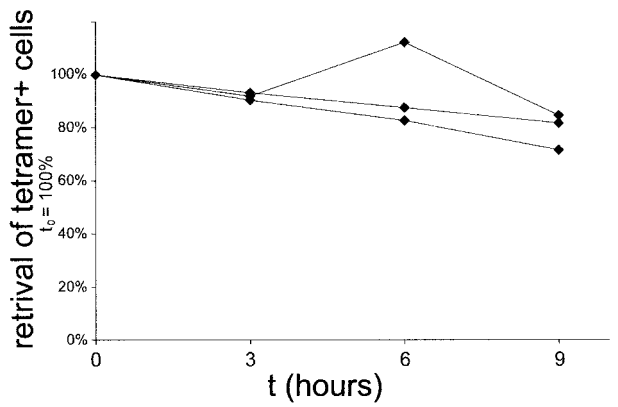

FIG. 4. Time-related variation of tetramer counts. Samples were stained by using the standard method, measured immediately (t = 0), and then stored on ice in the dark for the indicated times. Samples were measured in duplicate and the mean value was calculated. Values from different time points are given as a percentage of the values obtained at t = 0. Data from three independent experiments are presented.

Statistical Evaluation of the Assay-Related Variation

One of the aims of this study was to standardize experimental conditions, so that samples from different experiments could be compared. This is important if one wants to avoid variation due to freezing and thawing and other technical artifacts. To discern a true difference in cell counts from assay-dependent variation, we calculated different factors influencing the results. All samples were measured in duplicates, using one tube for the staining procedure and two different tubes for the acquisition. The overall standard deviation calculated with the use of these duplicates allows determination of between-tubes variation, which is influenced by the data acquisition, pipetting, and random distribution of the tetramer-positive cells. This standard deviations for the between-tubes variation were 3.67 cells/100 μl (10.18/10^5 $CD8^+$T cells, or 0.1%) for negative samples and 31.42 cells/100 μl (62.79 cells/10^5 $CD8^+$ T cells, or 0.63%) for positive samples. If one-fifth of the same tube was measured three times in a row (within-tube variation), a similar standard deviation was calculated (38.09 cells/100 μl; 92.15 cells/10^5 $CD8^+$ T cells, or 0.92%).

To calculate the physiologic range of tetramer-positive $CD8^+$ cells in healthy seropositive donors, we examined the same donors three times within 2 months. Of six donors, the mean range of variation was 28.6% (minimum, 16.6%; maximum, 43.0%, normalized for $CD8^+$ T-cell counts). This variation is attributed to the interassay variation plus the physiologic variation within the donor. These data are useful for further studies, because assay-to-assay variation for up to 50% must be attributed to physiologic and/or assay-related variations, whereas higher or lower values can be considered a true increase or a true decrease. Representative examples are shown in Figure 5.

Influence of Different Gating Strategies

It has been demonstrated in different studies that the quantitation of rare cells depends highly on different gating strategies (34–36). To determine this gating-related bias in our setting, we reanalyzed a set of data by using three different gating strategies (Fig. 1): we first compared the data obtained with our standard gating strategy (four colors, exclusion gate, method A) with data obtained by analysis of the same experiments without the use of the fourth color as an exclusion gate (method B). To compare the two methods, we determined the limits of agreement as suggested by Bland and Altman (33). As demonstrated in Figure 6, omitting the exclusion gate did not substantially change the standard method with regard to background staining (Fig. 6A and 6B, CMV^- donors). The number of $CD8^+$ cells was slightly increased (not shown), which we consider to be a minor variation. Thus, the fourth channel can be used for other purposes, e.g., characterization of the phenotype. As an alternative gating strategy, we analyzed our data by using the classic FSC/SSC lymphocyte gate, followed by a CD8/tetramer dot plot. This strategy resulted in similar values, with a slightly increased background (data not

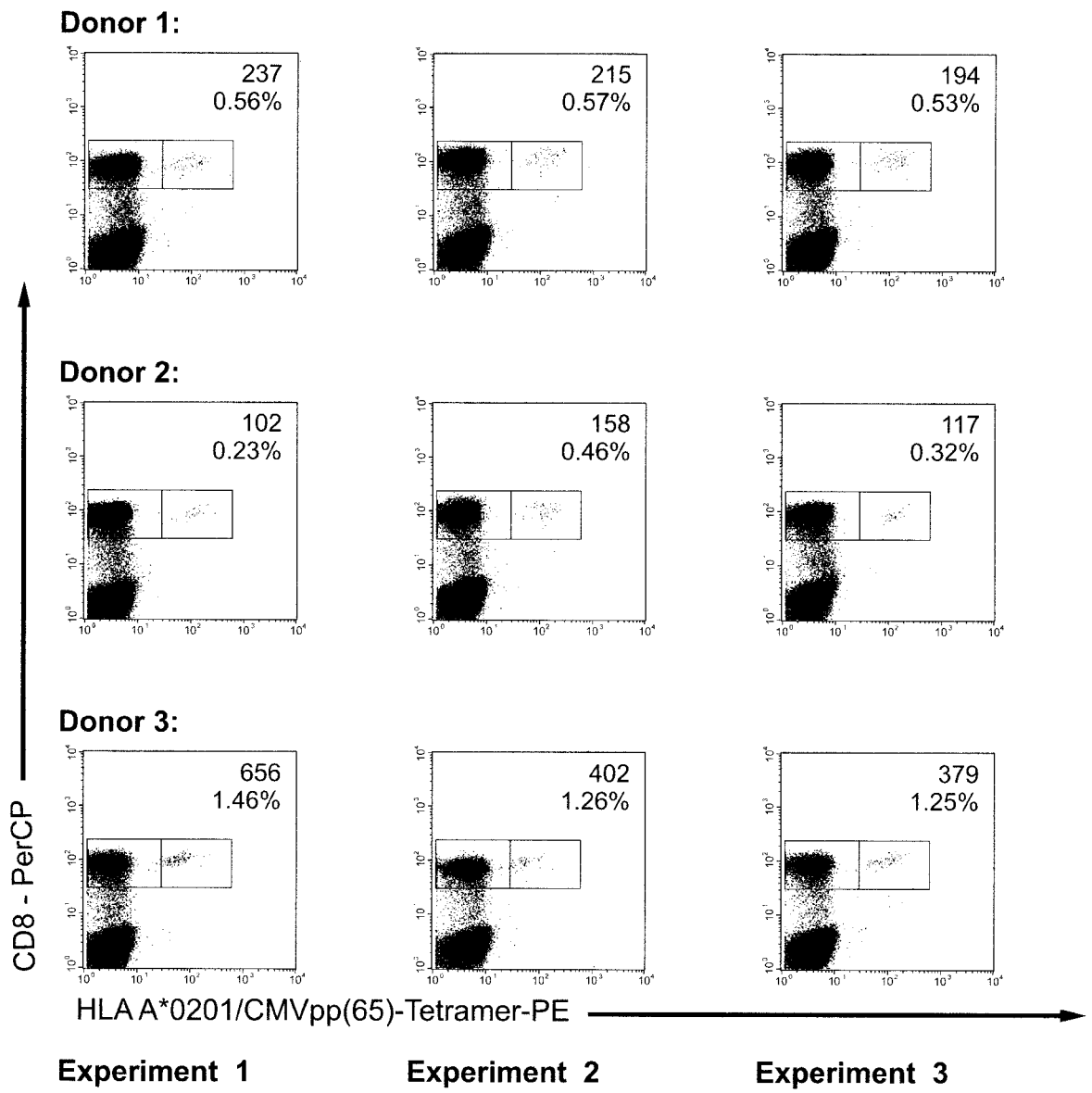

FIG. 5. Variation of tetramer-positive cell numbers from assay to assay and over time. The same donors were evaluated for the absolute number of tetramer-positive T cells on 3 different days within a 2-month period. Representative examples from three (of six) different CMV^+ donors are given. Numbers represent absolute numbers of tetramer-positive cells/100 μl whole blood (upper row) and percentage of $CD8^+$ T cells.

shown). One drawback of this analysis is the bias due to the use of the CD3 anchor during data acquisition and the high amplification of FSC and SSC. The preselection of $CD3^+$ cells makes it much easier to draw an appropriate FSC/SSC gate. In initial experiments using isolated peripheral blood mononuclear cells (PBMCs), cells were acquired without setting a threshold. The FSC/SSC turned out to be the source of the highest variation (data not shown).

Because light scatter parameters appear to be the major source for variability in gating, we wondered whether the analysis could be done without these parameters. We analyzed the data by gating on the $CD3^+FL4^-$ population in an FL1(CD3)/FL4(CD14,16,19,56) dot plot and displayed these cells in a tetramer/CD8 dot plot (method C). Figure 6 shows a substantial variation of background values and numbers of positive events in comparison with our standard method. Hence, light scatter parameters cannot be omitted.

The use of a CD45 anchor also has been suggested for the quantitation of $CD4^+$ cells in HIV^+ patients (8). We compared samples stained with CD45-APC as the fourth color with our standard staining method. Neither the exclusion gate nor the use of an additional CD45 anchor changed the number of tetramer-positive cells substantially (data not shown).

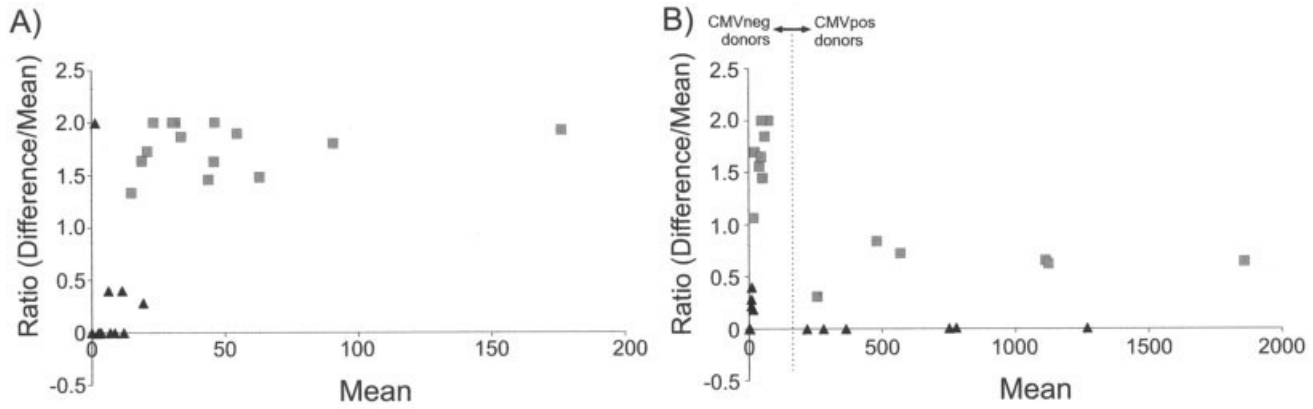

FIG. 6. Influence of different gating strategies. Cells were stained with the standard method: CD3-FITC/tetramer-PE/CD8-PerCP/(CD14/16/19/56-APC). Data were analyzed with three different methods (see Fig. 1). Method A: Standard method (see Fig. 1). Method B: Standard method without the FL4-exclusion channel. Method C: Gating on the FL1(CD3)$^+$/FL4$^-$ population and displaying these cells in an FL2(tetramer)/FL3(CD8) dot plot without the use of light scatter parameters. Let a_{1-n} be the values obtained by method A and b_{1-n} and c_{1-n} the values obtained by methods B and C, respectively. Triangles represent data obtained by comparison of methods A and B: x axis, mean of a_x and b_x; y axis, $(b_x - a_x)$/mean(a_x;b_x). Rectangles represent the corresponding data comparing method C with method A (33). **A:** Background staining obtained by staining with the HIV(pol) tetramer. Limits of agreement: method B versus A (triangles): mean (y value), 0.22; standard deviation, 0.54. Method C versus A (rectangles): mean, 1.77; standard deviation, 0.23. **B:** Staining with CMV(pp65) tetramer. Values to the left of the bar represent data obtained from CMV$^-$ donors. Values to the right represent data obtained from CMV$^+$ donors. Limits of agreement: method B versus A (triangles): mean (y value), 0.08; standard deviation, 0.14. Method C versus A (rectangles): mean, 1.22; standard deviation, 0.59.

DISCUSSION

The direct ex vivo quantitation of antigen-specific T cells provides an insight into the development and dynamics of T-cell responses in tumor immunology and infectious diseases (1). There are several methods to monitor antigen-specific cells, e.g., tetramer staining of the specific T-cell receptor, intracellular cytokine staining, and ELISPOT assays. These assays are complementary to each other. Assays such as cytokine staining or ELISPOT demonstrate the functional capacity of the cells but depend on in vitro restimulation. Tetramer staining demonstrates the phenotype, but not the function, of the cell.

The low frequencies of CD8$^+$ T cells specific for a given peptide antigen in the peripheral blood require highly accurate methods that depend on variables such as sample processing, viability, and background. Numbers are often given as a percentage of CD8$^+$ T cells alone, which is an additional source of variability. Variation from experiment to experiment often complicates the interpretation of the data. Freezing of the probes and analysis of all probes in one experiment are often performed, but variation due to the freezing and thawing process itself cannot be avoided.

In this study we have presented and evaluated a single-platform, four-color flow cytometric method for the determination of tetramer-positive cells from whole blood. The method is rapid—staining and analysis can be performed within 1 h after the blood is drawn—easy to perform, accurate, and produces results as events per volume of whole blood and as a percentage of CD8$^+$ cells. In patients with highly differing T-cell counts, e.g., in immunosuppressed patients, this additional information about the absolute numbers of tetramer-positive cells might better reflect the immunologic "power" of the T-cell response than the mere percentage of CD8$^+$ cells.

Several points have turned out to be critical for the performance of the assay. With the use of Trucount tubes, a defined volume of the probe can be determined, because the exact number of the beads per tube is known. Identifying the beads is easy because they show a bright fluorescence in all four channels. The manufacturers recommend the use of one tight gate in an FL1/FL2 dot plot. However, we found using at least three or, better, all four colors and combining the two regions into a "bead gate" to be more exact. This decreases the possibility that nonspecifically stained cells, aggregates of cells, or dead cells are counted as beads and allows for the use of larger regions, which avoids the exclusion of beads due to a gate that is too tight.

Another important feature is the use of an anchor marker for data acquisition. With a whole blood/no-wash method, the amount of platelets or debris is high. Acquisition of ungated (i.e., setting the threshold to 0) events results in large amounts of data that are difficult to handle and analyze. Selection before data acquisition needs to be done. We chose CD3 as an anchor, because it homogenously stains the T-cell population and is not expressed on B and natural killer cells that would also fall in an FSC/SSC lymphocyte gate. Setting the threshold so that CD3$^-$ events are excluded within the process of data acquisition helps to reduce the size of the FCS files.

The definition of gating parameters, especially for FSC, to exclude debris is often difficult. However, the use of light scatter parameters is necessary to achieve a low background, as demonstrated in Figure 6. We used three strategies to facilitate gating: (a) the use of a CD3 anchor for acquisition to exclude debris; (b) strong amplification of the light scatter parameters to focus on lymphocytes. Granulocytes and monocytes are not within the bound-

aries of the dot plot, but they ought to be excluded by gating, so this method is valid. (c) Using an FSC/CD8 density plot rather than the usual FSC/SSC plot defines the upper and lower borders of the FSC gate for the cells of interest, i.e., the highly $CD8^+$ population. If these cells are then displayed in an SSC/CD3 dot plot, gating on the T cell population is facilitated. Combination of these two regions takes into account the expression of CD3, CD8, and the typical light scatter appearance of lymphocytes.

It is much easier to standardize the sequential gating strategy when using square regions rather than polygonal regions and by combining each light scatter parameter with a fluorescence channel rather than using the classic FSC/SSC lymphocyte gate. Of the 25 experiments with approximately 300 samples, we only had to make slight adjustments for region 1 in one experiment and for region 4 in eight experiments (see Fig. 1). Variation using the classical FSC/SSC region was relatively low in our experiments when comparing different gating strategies, but because data were acquired with a CD3 anchor, debris and $CD3^-$ events were already excluded and gating was facilitated. Our own experience with ungated PBMCs and data from different groups showed that the light scatter appearance, especially FSC, contributes most to the gating-related variance (34–36). An additional gate to exclude all cells that are positive for other lineage markers can be used but is not a prerequisite for the successful identification of tetramer-positive cells. The fourth channel can serve for the characterization of the phenotype by using markers such as CD45RA, CD45RO, and CCR7 or activation markers. However, because the staining procedure is done at room temperature, caution is necessary when the cells are characterized for markers that are rapidly regulated after antibody-binding, e.g., via internalization.

Dead cells do not represent a major problem in this assay. In initial experiments, staining with amino actinomycin D (7-AAD) showed no significant numbers of dead cells within the $CD8^+$ population (data not shown). Because we used fresh whole blood and a CD3 anchor for acquisition, this is not surprising. The loss of tetramer-positive events after periods longer than 3 h on ice (Fig. 4) might be explained by activation and subsequent cell death due to binding of the T-cell receptor during the staining period at room temperature (37–39). Longer storage of the blood sample itself also might result in different staining characteristics, including a larger amount of dead cells, which could increase background staining. Switching to a system using CD8-APC in FL4 instead of CD8-PerCP and adding 7-AAD as a dye for dead cells in FL3 would resolve the problem.

We chose CMV infection as a model disease, because the T-cell response in healthy donors is robust and monitoring for CMV-specific cells has an impact in a variety of clinical settings, e.g., in patients receiving a liver, kidney, or bone marrow transplant (11,15,18–21,27). In a number of studies, quantitation of CMV-specific T cells was done with tetramers using PBMCs (14,20,21,24,26) or whole blood (17,22). In a recent study, Engstrand et al. analyzed CMV-specific T cells in healthy donors and immunosuppressed patients by using a similar method. In their work, three assays, tetramer staining and intracellular interferon-γ staining after pulsing with lysate or pp65 peptide, were compared by using a whole blood staining procedure with a subsequent lysing and washing step or a single-platform approach in some experiments. (25). Our data are consistent with the data presented in that study and in the studies mentioned above concerning the range of CMV responses in healthy donors. Some differences can be discussed in view of the different methodologies. For example, a dual-platform approach, including washing steps and different gating strategies, is usually used. The general focus in these studies is the monitoring of immunosuppressed patients. Our study focused on issues of background staining, standardization of the gating procedure, and statistical analysis of assay-related variation by analyzing various variables possibly influencing assay accuracy. Therefore it provides complementary data to the aforementioned studies and might be useful for the design of future studies.

The method presented here is applicable to a variety of infectious diseases, autoimmune diseases, or tumor immunology provided that the immunogenic epitope of the antigen in question is known. Due to the small amount of blood required (500 μl is needed for duplicates and controls), it is a useful tool, especially for analysis in pediatric patients.

The detection limit of the method based on our data is 14 cells/100 μl whole blood, which equals approximately 0.04% of all $CD8^+$ T cells. This is slightly higher than the currently accepted detection limit (0.01%) (1). The difference can be explained by the statistical method used to determine the upper threshold limit. Most negative controls in our study had very low background values (mean 50% quantile: 1.58 cells/100 μl; 0.003% of the $CD8^+$ T cells; Table 1). Because a normal distribution of these values could not be assumed, the calculation of a mean value and its standard deviation was not possible. We therefore calculated the 99% quantile for each donor separately and chose the donor with the highest individual 99% quantile to define the detection limit to clearly identify only truly positive cell populations.

Establishing a general background threshold is advantageous because, for further studies, a positive sample can now be defined as a sample with a cell count higher than this defined background and is valid only if the corresponding negative control (e.g., stained with HIV tetramer) lies within this interval. Further, information concerning between-tubes variation can be used as an additional tool to validate the assay. This strategy ensures that only samples with a similar background staining are compared, and these data do not need to be recalculated by subtracting the background.

Choosing the appropriate negative control is crucial. We chose HIV(pol) as a control, which is commonly used as a negative control in various assays (e.g., ELISPOT or intracellular cytokine staining). The data obtained for the background were confirmed by the data obtained from

samples of HLA-A*0201$^+$/CMV$^-$ donors that were stained with the CMV tetramer. However, in experimental settings where a very low frequency of specific T cells is expected, the use of tetramers with different alleles may be useful.

The knowledge about the normal (physiologic and assay-related) variations from experiment to experiment facilitates the comparison of data obtained from different time points. This helps to interpret data about an increase or a decrease in patient cohorts and reduces the risk of over-interpretation of slight changes (in our case, $<$50%) of the tetramer-positive T-cell counts.

A major advantage of tetramer staining is that it is a straightforward technique to identify antigen-specific cells. One limitation of tetramer technology is its restriction for specific HLA alleles and certain antigen epitopes. Combining tetramer staining with functional assays provides additional information, and the latter can be used if the immunogenic epitope is not clearly defined.

The method evaluated in this study reduces processing time and handling to a minimum and is close to the in vivo setting. Sample processing, data acquisition, and analysis are standardized; therefore, results from different laboratories might be easier to compare. The method provides a robust, precise, time-efficient, and standardized assay to be used as a tool to understand the development and expansion of the T-cell pool.

ACKNOWLEDGMENTS

We thank U. Schlütter for expert technical assistance. S.S. was supported by Köln Fortune. This work is part of his thesis. D.H.B. was supported by the Clinical Cooperation Vaccinology.

LITERATURE CITED

1. Yee C, Greenberg P. Modulating T-cell immunity to tumours: new strategies for monitoring T-cell responses. Nat Rev Cancer 2002;2: 409–419.
2. Klenerman P, Cerundolo V, Dunbar PR. Tracking T cells with tetramers: new tales from new tools. Nat Rev Immunol 2002;2:263–272.
3. Strike P. Measurement in laboratory medicine: a primer on control and interpretation. Oxford: Butterworth-Heinemann; 1996.
4. Brecher ME, Sims L, Schmitz J, Shea T, Bentley SA. North American Multicenter Study on flow cytometric enumeration of CD34+ hematopoietic stem cells. J Hematother 1996;5:227–236.
5. Gratama JW, Orfao A, Barnett D, Brando B, Huber A, Janossy G, et al. Flow cytometric enumeration of CD34+ hematopoietic stem and progenitor cells. European Working Group on Clinical Cell Analysis. Cytometry 1998;34:128–142.
6. Gratama JW, Sutherland DR, Keeney M. Flow cytometric enumeration and immunophenotyping of hematopoietic stem and progenitor cells. Semin Hematol 2001;38:139–147.
7. Sutherland DR, Anderson L, Keeney M, Nayar R, Chin-Yee I. The ISHAGE guidelines for CD34+ cell determination by flow cytometry. International Society of Hematotherapy and Graft Engineering. J Hematother 1996;5:213–226.
8. Schnizlein-Bick CT, Mandy FF, O'Gorman MR, Paxton H, Nicholson JK, Hultin LE, et al. Use of CD45 gating in three and four-color flow cytometric immunophenotyping: guideline from the National Institute of Allergy and Infectious Diseases, Division of AIDS. Cytometry 2002;50:46–52.
9. Bergeron M, Faucher S, Ding T, Phaneuf S, Mandy F. Evaluation of a universal template for single-platform absolute T-lymphocyte subset enumeration. Cytometry 2002;50:62–68.
10. Brocklebank AM, Sparrow RL. Enumeration of CD34+ cells in cord blood: a variation on a single-platform flow cytometric method based on the ISHAGE gating strategy. Cytometry 2001;46:254–261.
11. Kern F, Bunde T, Faulhaber N, Kiecker F, Khatamzas E, Rudawski IM, et al. Cytomegalovirus (CMV) phosphoprotein 65 makes a large contribution to shaping the T cell repertoire in CMV-exposed individuals. J Infect Dis 2002;185:1709–1716.
12. Burak KW, Kremers WK, Batts KP, Wiesner RH, Rosen CB, Razonable RR, et al. Impact of cytomegalovirus infection, year of transplantation, and donor age on outcomes after liver transplantation for hepatitis C. Liver Transpl 2002;8:362–369.
13. Fontana I, Verrina E, Timitilli A, Arcuri V, Basile G, Losurdo G, et al. Cytomegalovirus infection in pediatric kidney transplantation. Transplant Proc 1994;26:18–19.
14. Hassan-Walker AF, Vargas Cuero AL, Mattes FM, Klenerman P, Lechner F, Burroughs AK, et al. CD8+ cytotoxic lymphocyte responses against cytomegalovirus after liver transplantation: correlation with time from transplant to receipt of tacrolimus. J Infect Dis 2001;183: 835–843.
15. Sester M, Sester U, Gartner B, Heine G, Girndt M, Mueller-Lantzsch N, et al. Levels of virus-specific CD4 T cells correlate with cytomegalovirus control and predict virus-induced disease after renal transplantation. Transplantation 2001;71:1287–1294.
16. Singhal S, Shaw JC, Ainsworth J, Hathaway M, Gillespie GM, Paris H, et al. Direct visualization and quantitation of cytomegalovirus-specific CD8+ cytotoxic T-lymphocytes in liver transplant patients. Transplantation 2000;69:2251–2259.
17. Engstrand M, Tournay C, Peyrat MA, Eriksson BM, Wadstrom J, Wirgart BZ, et al. Characterization of CMVpp65-specific CD8+ T lymphocytes using MHC tetramers in kidney transplant patients and healthy participants. Transplantation 2000;69:2243–2250.
18. Chen FE, Aubert G, Travers P, Dodi IA, Madrigal JA. HLA tetramers and anti-CMV immune responses: from epitope to immunotherapy. Cytotherapy 2002;4:41–48.
19. Aubert G, Hassan-Walker AF, Madrigal JA, Emery VC, Morte C, Grace S, et al. Cytomegalovirus-specific cellular immune responses and viremia in recipients of allogeneic stem cell transplants. J Infect Dis 2001;184:955–963.
20. Gratama JW, van Esser JW, Lamers CH, Tournay C, Lowenberg B, Bolhuis RL, Cornelissen JJ. Tetramer-based quantification of cytomegalovirus (CMV)-specific CD8+ T lymphocytes in T-cell–depleted stem cell grafts and after transplantation may identify patients at risk for progressive CMV infection. Blood 2001;98:1358–1364.
21. Benz C, Utermohlen O, Wulf A, Villmow B, Dries V, Goeser T, et al. Activated virus-specific T cells are early indicators of anti-CMV immune reactions in liver transplant patients. Gastroenterology 2002; 122:1201–1215.
22. He XS, Rehermann B, Boisvert J, Mumm J, Maecker HT, Roederer M, et al. Direct functional analysis of epitope-specific CD8+ T cells in peripheral blood. Viral Immunol 2001;14:59–69.
23. Gratama JW, Cornelissen JJ. Diagnostic potential of tetramer-based monitoring of cytomegalovirus-specific CD8+ T lymphocytes in allogeneic stem cell transplantation. Clin Immunol 2003;106:29–35.
24. Cwynarski K, Ainsworth J, Cobbold M, Wagner S, Mahendra P, Apperley J, et al. Direct visualization of cytomegalovirus-specific T-cell reconstitution after allogeneic stem cell transplantation. Blood 2001; 97:1232–1240.
25. Engstrand M, Lidehall AK, Totterman TH, Herrman B, Eriksson BM, Korsgren O. Cellular responses to cytomegalovirus in immunosuppressed patients: circulating CD8+ T cells recognizing CMVpp65 are present but display functional impairment. Clin Exp Immunol 2003; 132:96–104.
26. Gamadia LE, Rentenaar RJ, Baars PA, Remmerswaal EB, Surachno S, Weel JF, et al. Differentiation of cytomegalovirus-specific CD8(+) T cells in healthy and immunosuppressed virus carriers. Blood 2001; 98:754–761.
27. Li CR, Greenberg PD, Gilbert MJ, Goodrich JM, Riddell SR. Recovery of HLA-restricted cytomegalovirus (CMV)–specific T-cell responses after allogeneic bone marrow transplant: correlation with CMV disease and effect of ganciclovir prophylaxis. Blood 1994;83:1971–1979.
28. Altman JD, Moss PA, Goulder PJ, Barouch DH, McHeyzer-Williams MG, Bell JI, et al. Phenotypic analysis of antigen-specific T lymphocytes. Science 1996;274:94–96.
29. Busch DH, Pilip IM, Vijh S, Pamer EG. Coordinate regulation of complex T cell populations responding to bacterial infection. Immunity 1998;8:353–362.
30. McMichael AJ, O'Callaghan CA. A new look at T cells. J Exp Med 1998;187:1367–1371.
31. Schatz PJ. Use of peptide libraries to map the substrate specificity of a peptide-modifying enzyme: a 13 residue consensus peptide specifies biotinylation in *Escherichia coli*. Biotechnology (NY) 1993;11: 1138–1143.

32. Overton WR. Modified histogram subtraction technique for analysis of flow cytometry data. Cytometry 1988;9:619–626.
33. Bland JM, Altman DG. Measuring agreement in method comparison studies. Stat Methods Med Res 1999;8:135–160.
34. Chang A, Ma DD. The influence of flow cytometric gating strategy on the standardization of CD34+ cell quantitation: an Australian multicenter study. Australasian BMT Scientists Study Group. J Hematother 1996;5:605–616.
35. Gratama JW, Kraan J, Keeney M, Granger V, Barnett D. Reduction of variation in T-cell subset enumeration among 55 laboratories using single-platform, three or four-color flow cytometry based on CD45 and SSC-based gating of lymphocytes. Cytometry 2002;50:92–101.
36. Bergeron M, Nicholson JK, Phaneuf S, Ding T, Soucy N, Badley AD, et al. Selection of lymphocyte gating protocol has an impact on the level of reliability of T-cell subsets in aging specimens. Cytometry 2002; 50:53–61.
37. Knabel M, Franz TJ, Schiemann M, Wulf A, Villmow B, Schmidt B, et al. Reversible MHC multimer staining for functional isolation of T-cell populations and effective adoptive transfer. Nat Med 2002;8:631–637.
38. Xu XN, Purbhoo MA, Chen N, Mongkolsapaya J, Cox JH, Meier UC, et al. A novel approach to antigen-specific deletion of CTL with minimal cellular activation using alpha3 domain mutants of MHC class I/peptide complex. Immunity 2001;14:591–602.
39. Whelan JA, Dunbar PR, Price DA, Purbhoo MA, Lechner F, Ogg GS, et al. Specificity of CTL interactions with peptide-MHC class I tetrameric complexes is temperature dependent. J Immunol 1999;163:4342–4348.